Quantitative breast density in Contrast-Enhanced Mammography

Gisella Gennaro (gisella.gennaro@iov.veneto.it)
Veneto Institute of Oncology (IRCCS) https://orcid.org/0000-0003-2444-1778
Melissa L. Hill
Volpara Health Technologies
Elisabetta Bezzon
Veneto Institute of Oncology Institute for Hospitalization and Care Scientific: Istituto Oncologico Veneto Istituto di Ricovero e Cura a Carattere Scientifico
Francesca Caumo
Veneto Institute of Oncology Institute for Hospitalization and Care Scientific: Istituto Oncologico Veneto Istituto di Ricovero e Cura a Carattere Scientifico

Research article

Keywords: Breast density, Mammography, Dual Energy, Contrast-Enhanced

Posted Date: April 9th, 2021

DOI: https://doi.org/10.21203/rs.3.rs-400818/v1

Abstract

Background: Breast density is an independent risk factor for breast cancer, and cancer detection in mammography is reduced in dense breasts. Quantitative tools are available to measure breast density from digital mammography (DM) or tomosynthesis (DBT). Contrast-enhanced mammography (CEM) is an emerging breast imaging technique, consisting of the acquisition of an image pair (low-energy, LE, and high-energy, HE) for each mammography view. LE-CEM images have been demonstrated to be visually equivalent to a standard mammogram, thereby, CEM examinations do not require additional mammography to complete the clinical information. In this study, volumetric breast density (VBD) measured in LE-CEM was compared with VBD obtained from DM/DBT images.

Methods: Between Mar 2019 and Dec 2020 222 women were enrolled in a prospective clinical trial aiming to compare clinical performance of CEM with breast MRI in a population of women at intermediate and high risk for breast cancer. In this observational cohort study, 150 women enrolled in this trial having at least a DM/DBT study performed before/after CEM were selected. CEM and previous/subsequent DM/DBT images were processed by an automatic algorithm to calculate VBD for each view. VBD from LE-CEM and DM/DBT views were compared using a paired Wilcoxon test. $P < 0.05$ was considered indicative of a statistically significant difference. A multivariate regression model was applied to analyze the relationship between paired VBD differences and multiple independent variables certainly or potentially affecting VBD.

Results: Mean age of women included in this study was 51.0±8.4 years. Median VBD was comparable for LE-CEM and previous/subsequent DM/DBT (12.73% vs. 12.39%), not evidencing any statistically significant difference (P = 0.5855). VBD differences between LE-CEM and DM were associated to significant differences of glandular volume, breast thickness, compression force and pressure, contact area, and nipple-to-posterior-edge distance i.e. variables reflecting differences in breast positioning (coefficient of determination 0.6023; multiple correlation coefficient 0.7761).

Conclusions: Volumetric breast density can be obtained from low-energy contrast-enhanced spectral mammography and is not significantly different from volumetric breast density measured from standard mammograms.

Background

The term “breast density” indicates the proportion of fibroglandular to fatty breast tissue that can be derived from mammography imaging. It has been proven that clinical performance of mammography screening decreases as breast density increases, limiting the cancer detection rate while increasing the number of interval cancers [1, 2]. Furthermore, breast density has gained increasing attention as breast cancer risk factor [3, 4], and is considered a potential individual biomarker to be included in breast cancer predicting models [5–9]. Because of this twofold role of breast density as masking and risk factor, there is a strong debate to change the “one fits all” mammography screening model into “personalized”

screening models, i.e. screening programs including supplemental imaging for women with dense breasts or at increased risk for breast cancer [10–12].

Breast density can be evaluated using either human- or computer-based methods. Human-derived breast density is usually assessed by means of categorical variables, for instance BIRADS breast density [13], but is unavoidably affected by inter- and intra-observer variability [14, 15]. There are several computer-based methods using semi-automatic or fully automatic algorithms, capable of computing breast density as a percentage of breast area or breast volume [16–18]. Volumetric breast density (VBD), i.e. the percentage volume of fibroglandular tissue in the whole breast volume as computed by automatic software tools measured from digital mammograms, has been included into statistical models used to estimate individual risk of breast cancer [9, 19]. As mammography is progressively being replaced by digital breast tomosynthesis (DBT), the same tools have been adapted to calculate VBD from tomosynthesis projection images [20].

Contrast-enhanced mammography (CEM, also called contrast-enhanced digital mammography, CEDM, or contrast-enhanced spectral mammography, CESM) is a dual-energy subtraction technique [21–24] applied to breast imaging, which is showing potential in personalized screening models [25, 26]. In CEM, a pair of low-energy (LE) and high-energy (HE) images are acquired after contrast administration and used to construct the final “subtraction” image. The LE-CEM image is used to get the morphological information as for a standard mammogram, while the subtraction image provides the functional information enhancing in areas of contrast uptake by possible breast lesions [24, 27, 28]. In a multireader study, Fallenberg et al. demonstrated that there is no added clinical value in combining CEM with standard digital mammography (DM), and that the combination of CEM + DM just increases radiation dose, in particular for dense breasts [29]. Superiority of CEM over standard digital mammography (DM) has been proven [30–32]. More importantly, CEM was proven to be comparable with breast MRI in local staging of breast cancer [29, 33], in therapy response assessment [24, 34], in management of symptomatic women [35], as problem solver in screening workup [36, 37]. Nevertheless, CEM has also shown its potential as a screening tool, above all for women with dense breasts [38] and/or increased risk for breast cancer [39, 40]. The prospective of using CEM as a detection tool requires that breast density can be obtained directly from CEM images. In this study, volumetric breast densities measured from LE-CEM images obtained within a study population of women at increased breast cancer risk was compared with those measured from mammography or tomosynthesis acquired before or after the CEM exam. The study purpose was to figure out if quantitative breast density derived from LE-CEM can be successfully used to feed breast cancer risk models within personalized screening protocols.

Materials And Methods

Study design and population

This observational cohort study (single-center) was approved by the institutional Ethics Committee. The study population included women enrolled from March 2019 to December 2020 in a prospective clinical

trial (CE IOV #2017/92) comparing clinical performance of CEM with breast MRI in a population of 300–500 women at intermediate and high risk for breast cancer. Signed informed consents together with a questionnaire to gather the information required by the Tyrer-Cuzick breast cancer risk model were obtained from all women enrolled in the prospective trial. For women without known BRCA1 or BRCA2 mutations, the lifetime risk was calculated using the IBIS freeware software that implements v. 8.0 of the Tyrer-Cuzick model [41]; according to the NICE Guideline on familial breast cancer, enrolled women were classified at high risk for breast cancer if their lifetime risk was above 30%, and at intermediate risk if their lifetime risk was between 17% and 30% [42].

Subject selection for this observational study was exclusively based on the availability of mammography or DBT acquired before or after CEM. A total of 150 women with previous/subsequent mammography or DBT were used in this analysis.

CEM and mammography/tomosynthesis imaging

Contrast-enhanced mammography was performed by a GE Senographe Pristina unit (GE Healthcare, Milwaukee Wis) after injection of 1.5 mL/kg iodinated contrast agent (GE Omnipaque 350) using an automatic injector (2.5 ml/s). For pre-menopausal or peri-menopausal women, the examination was timed according to the phase of the woman's menstrual cycle to minimize potential MRI false positives and possible background parenchymal enhancement. A two-view (cranio-caudal, CC, and medio-lateral oblique, MLO) bilateral examination was performed starting two minutes after the contrast agent injection. For each mammography view, an image pair was acquired: (1) a low-energy image (LE-CEM) obtained using the same spectra as used for a standard mammography, such that most x-ray photons have energies below the absorption peak of the contrast agent (33.2 keV for iodinated contrast); (2) a HE image (HE-CEM) using copper filtration and tube voltage such as the resulting spectrum includes photons mostly above the iodine k-edge. As previously mentioned, the LE-image and a contrast-enhanced subtraction image obtained recombining LE-CEM and HE-CEM are used for diagnosis [24, 28]. Figure 1 shows a scheme of CEM acquisition and an example of CEM images used for diagnosis.

Figure 1

(a) CEM acquisition. Two minutes after the administration of iodinated contrast agent, for each mammography view an image pair is acquired: a low-energy image (LE-CEM) using an x-ray spectrum similar to that used to obtain a standard mammogram, and a high-energy image (HE-CEM) using a spectrum obtained with appropriate filtration and high tube voltage such as photon energies are mostly above the iodine k-edge (33.2 keV). (b) CEM interpretation. The LE-CEM is used for the morphological information and the contrast-enhanced subtraction image used as functional imaging; the HE-CEM image is not useful for diagnosis.

The subtracted CEM images were visually assessed by an experienced radiologist for contrast agent uptake in the normal tissue, or background parenchymal enhancement (BPE), and assigned one of four categories: minimal, mild, moderate, or marked [48].

The DM/DBT exams were collected from among the conventional exams that were closest in time to the acquisition date of the CEM study. This may have been prior to or following the CEM exam date. Mammography examinations were acquired by one of the following digital units: GE Senographe DS, GE Senographe Essential, GE Senographe Pristina (the same equipment used for CEM), Hologic Selenia Dimensions, IMS Giotto Image 3DL, Siemens Mammomat Inspiration. Tomosynthesis examinations were obtained either by GE Senographe Pristina or by Hologic Selenia Dimensions.

Breast density

In this study, VBD was calculated by Volpara v. 1.5.5.1 (Volpara Health Ltd., Wellington, New Zealand) in a research mode to allow processing of CEM images. The Volpara algorithm uses a model of the physics of digital mammography to work backwards from the unprocessed image pixel value to the amounts of fibroglandular and adipose tissues that would result in the measured x-ray attenuation at each detector element location. The total breast volume is generated using the compressed breast thickness reported in the image DICOM header and a model for the shape of the breast. Using this estimated breast volume and the fibroglandular tissue volume derived from the x-ray attenuation the VBD value (Fibroglandular Tissue Volume / Volume of Breast) is calculated [16]. For CEM examinations VBD computing was limited to the LE-images. To help explain potential sources of density variability, other parameters studied for their potential association with VBD are breast thickness and compression force (both obtained from the image DICOM header), area of the compression paddle in contact with the breast [43] and distance between nipple and the posterior-edge (both determined by image analysis) [44], compression pressure calculated as the ratio between compression force and contact area, and mean glandular dose (MGD) obtained by applying the dosimetry model proposed by Dance and colleagues [45–47].

Statistical analysis

VBD values obtained from LE-CEM and DM/DBT paired views were compared using a two-tailed Wilcoxon test. $P < 0.05$ was considered statistically significant. The same test was applied to any other variable listed above certainly or potentially affecting VBD values. Correlation between VBD measured from LE-CEM views and VBD measured from previous/subsequent DM/DBT views was evaluated by estimating the Spearman correlation coefficient, while the level of agreement between the two VBD datasets was explored thorough Bland-Altman plots. The same analysis (correlation and Bland-Altman) was performed for each patient case, after having averaged paired VBD values from available views (CC and MLO) for the two datasets.

Finally, after having obtained two paired per-patient datasets by averaging per-view VBDs and any other considered variable, the absolute difference was calculated between mean VBD obtained from CEM and previous/subsequent DM/DBT, as well as between any mean differences between all the other variables. A multiple regression model was then applied to analyze the relationship between the dependent variable “VBD difference” and the differences between any other variable considered independent. The regression model was weighted for 1/(VBD difference variance) to correct for heteroscedasticity.

Per-case VBD difference was also evaluated as a function of BPE assessed from CEM. VBD difference between the two subgroups showing minimal or mild BPE and moderate or marked BPE was compared with a Mann-Whitney test for independent samples, using the same 0.05 significance level.

Statistical analysis was performed using MedCalc® Statistical Software version 19.7 (MedCalc Software Ltd, Ostend, Belgium; https://www.medcalc.org; 2021).

Results

Study population

Volumetric breast density from 150 CEM examinations were compared with digital mammography or tomosynthesis performed either before or after CEM. On average, prior DM/DBT were obtained 10.8 months before or after the CEM examination; median time interval was 12 months, 91% of cases (134/150) had mammography or tomosynthesis ±15 months before/after CEM.

Table 1 shows characteristics of study population, including age, menopausal status, risk category, and breast density category.

Table 1
Characteristics of study population

Characteristic	Values
Number of women	150
Age (y)	51.0±8.8
mean±SD	51
median	(35, 76)
range	
Menopausal status	68 (45.33%)
Premenopausal	14 (9.33%)
Perimenopausal	68 (45.33%)
Postmenopausal	
Risk category	30 (20.00%)
BRCA1	36 (24.00%)
BRCA2	62 (41.33%)
HIGH (lifetime risk > 30%)	22 (14.67%)
INTERMEDIATE (lifetime risk > 17% & ≤30%)	
BIRADS breast density category	9 (6.00%)
Predominantly fatty (A)	27 (18.00%)
Scattered fibroglandular (B)	55 (36.67%)
Heterogeneously dense (C)	59 (39.33%)
Extremely dense (D)	
Background parenchymal enhancement (BPE)	65 (43.33%)
Minimal	44 (29.33%)
Mild	38 (25.33%)
Moderate	3 (2.00%)
Marked	
Previous/subsequent exam	120 (80.00%)
Mammography	30 (20.00%)
Tomosynthesis	

BI-RADS Breast Imaging-Reporting and Data System, BRCA1/BRCA2 women with a mutation of the BRCA1 or BRCA2 genes, SD standard deviation

Mean age was 51.0±8.8 years, ranging between 35 and 76 years. Pre-menopausal women were 45.33% (68/150) of enrolled women, while remaining 54.67% (82/150) were either peri- (14/150 = 9.33%) or post-menopausal (68/150 = 45.33%). Most of subjects enrolled in the study were high-risk women (128/150 = 85.33%); 44.00% (66/150) had proven BRCA1 or BRCA2 mutation, and 41.33% (62/150) had family history of breast cancer that, together with other risk factors, including also VBD, lead to lifetime risk for breast cancer above 30%. The remaining 14.67% of women (22/150) had intermediate risk (lifetime risk between 17% and 30%). Women included in the study population had mostly dense breasts: 76.00% (114/150) classified BIRADS C or D, and 24.00% (36/150) classified BIRADS A or B. Regarding the parenchymal background enhancement evaluated with CEM, 72.67% of women showed minimal or mild BPE (109/150), and 27.3% moderate or marked (41/150). Previous or subsequent exams compared to CEM were 80% (120/150) DM and 20% (30/150) DBT.

Volumetric breast density

Table 2 shows results from the Wilcoxon paired test for VBD and all the other variables considered measured from LE-CEM and DM/DBT paired views.

Table 2
Comparison between CEM and DM/DBT of volumetric breast density and related variables.

Variable	LE-CEM median	DM/DBT median	Hodges-Lehmann median difference	95% confidence interval	P-value
VBD (%)	12.73	12.39	0.075	-0.19 to 0.34	0.5855
Breast volume (cm^3)	508.15	534.57	25.58	18.89 to 32.98	< 0.0001
Glandular volume (cm^3)	55.90	59.44	3.315	1.975 to 4.660	< 0.0001
Breast thickness (mm)	47.7	50.0	2.35	1.90 to 2.80	< 0.0001
Compression force (N)	102	85	-15.0	-17.5 to -12.0	< 0.0001
Compression pressure (kPa)	11.83	10.46	1.655	-1.995 to 1.310	< 0.0001
Contact area (mm^2)	8529.46	8311.63	-144.14	-222.61 to -68.77	0.0003
Nipple distance from posterior edge (mm)	88.40	88.80	0.60	0.10 to 1.15	0.0180
Mean glandular dose (mGy)	1.544	1.527	-0.043	-0.074 to -0.012	0.0083

Median values obtained from LE-CEM and DM/DBT paired views, Hodges-Lehmann median difference and 95% confidence interval, and P-value from the Wilcoxon paired test for VBD and all available variables actually or potentially associated to VBD calculation.

CEM contrast-enhanced mammography, DM digital mammography, DBT digital breast tomosynthesis, VBD volumetric breast density

Median VBD was comparable for LE-CEM and previous/subsequent DM/DBT (12.73% vs. 12.39%), not evidencing any statistically significant difference ($P = 0.5855$). Conversely, median differences between any other variable pairs were statistically significant ($P < 0.05$).

Figure 2 shows the correlation plot (on the left) and the Bland-Altman plot (on the right) for VBD measured from LE-CEM and previous/subsequent DM/DBT exams, for single views (upper plots) and for individual cases obtained averaging VBD values from multiple views (bottom plots).

Figure 2

Figure 2: (a) Correlation plot of VBD measured in paired views obtained from LE-CESM and previous/subsequent DM/DBT exams; the Pearson's correlation coefficient was r = 0.87, a reduction of correlation can be noticed as VBD increases, especially for MLO views. (b) Bland-Altman plot of VBD difference between LE-CESM and previous/subsequent DM/DBT for each paired view; the mean difference was zero, the limits of agreement ±8%. (c) Correlation plot of mean VBD obtained by averaging single-view VBDs for each paired study obtained with LE-CESM and DM/DBT; the Pearson's correlation coefficient was r = 0.92, the heat map shows that VBD values were mostly grouped below 15%. (d) Bland-Altman plot of VBD difference between LE-CESM and previous/subsequent DM/DBT for each paired study; the mean difference was confirmed to be very close to zero, the limits of agreement reduced to ±5%.

The correlation was good for both per-view and per-case comparison (r = 0.87 and r = 0.92, respectively). In per-case analysis the correlation was slightly improved compared to per-view analysis because some VBD differences for specific views were attenuated by the averaging across multiple views belonging to the same study. The same effect was confirmed by the Bland-Altman plot: in both per-view and per-case plots the mean VBD difference is zero, but the limits of agreement were narrower in per-case than in per-view analysis (about ±6% against ±8%). From per-view plots it can be noticed that the largest VBD differences between LE-CEM and previous/subsequent DM/DBT images predominantly occurred for MLO views. The heat map in the per-case regression plots shows that volumetric breast density values were mostly below 15%. The VBD difference between LE-CEM and previous/subsequent DM/DBT tends to increase with breast density.

Multiregression analysis

Least squares multiple regression (weighted for variance) using per-case dataset showed that breast density variability between CEM and mammography/tomosynthesis was affected by all variables that one can consider to be reflecting differences in breast positioning, with the exclusion of breast volume. The sample case in Fig. 3 shows in the upper part the LE-CEM images of a woman with large fatty breasts, and in the lower part the prior mammograms acquired 12 months before: there is a large difference in breast volumes between the two examinations (CEM: 2634 cm^3; DM: 2058 cm^3; difference 576 cm^3) associated to large difference in breast positioning (CEM mean nipple-to-posterior-edge distance: 174 mm; DM: 156 mm; 18 mm difference), not producing significant variation in volumetric breast density (CEM: 1.9%; DM: 2.7%). Differently, the second sample case in Fig. 4 shows in the upper part LE-CEM images and in the lower part the subsequent (11.5 months later) mammography of a woman with dense breasts; mean VBD changes from 20.1–30.5% because of a better positioning in the second exam. In subsequent mammography breasts were better positioned, including about 1 cm more (nipple-to-posterior-edge distance) compared to CEM resulting in larger volume of fibroglandular tissue (136 cm^3 vs. 64 cm^3 with CEM) and larger overall breast volume (450 cm^3 vs. 319 cm^3 with CEM).

Figure 3

Figure 3: (Upper row) LE-CEM images of a woman with large fatty breasts. VBD: 1.9%; breast volume: 2634 cm^3; volume of glandular tissue: 51 cm^3; breast thickness: 85 mm; nipple-to-posterior-edge distance: 174 mm. (Lower row) DM images acquired 12 months before the CEM exam. VBD: 2.7%: breast volume: 2058 cm^3; volume of glandular tissue: 54 cm^3; breast thickness: 76 mm; nipple-to-posterior-edge distance: 155 mm. Despite the visible difference in breast positioning, the large reduction in breast volume due to worse positioning in the DM exam did not produce a significant variation of breast density, being the breasts predominantly fatty.

Figure 4

Figure 4: (Upper row) LE-CEM images of a woman with dense breasts. VBD: 20.1%; breast volume: 319 cm^3; volume of glandular tissue: 64 cm^3; breast thickness: 32 mm; nipple-to-posterior-edge distance: 86 mm. (Lower row) DM images acquired 11.5 months after the CEM exam. VBD: 30.5%; breast volume: 450 cm^3; volume of glandular tissue: 136 cm^3; breast thickness: 41 mm; nipple-to-posterior-edge distance: 98 mm. Breast positioning is better in DM exam, including an additional volume of glandular tissue leading to a significant increment in VBD.

As reported in Table 3, a VBD difference between LE-CEM and DM/DBT was associated to significant differences of glandular volume, breast thickness, compression pressure, nipple-to-posterior-edge distance, and to differences of compression force and contact area, while *P*-values for breast volume and MGD difference were above 0.05. The coefficient of determination (R^2) was 0.6023, while the multiple correlation coefficient was 0.7761.

Table 3
Coefficients of the regression equation and P-values resulting from the multiple regression model.

Independent variable difference	**Regression Coefficient**	***P*-value**
(Constant)	0.1741	
Breast volume (cm^3)	0.005017	0.1311
Glandular volume (cm^3)	+ 0.1174	**< 0.0001**
Breast thickness (mm)	-0.2748	**< 0.0001**
Compression force (N)	0.05008	**0.0036**
Compression pressure (kPa)	-0.5031	**0.0001**
Contact area (mm^2)	-0.0009143	**< 0.0001**
Nipple-to-posterior-edge distance (mm)	-0.1453	**0.0011**
Mean glandular dose (mGy)	-0.1373	0.6684

VBD difference between LE-CEM and DM/DBT was considered the dependent variable; difference in breast volume, glandular volume, breast thickness, contact area, compression force, compression pressure, nipple-to-posterior-edge distance, and mean glandular dose were included in the model as independent variables.

CEM contrast-enhanced mammography, DM digital mammography, DBT digital breast tomosynthesis, VBD volumetric breast density

Figure 5 provides a scatter plot matrix of the VBD differences and the differences between all the independent variables measured in the paired LE-CESM and DM/DBT cases. A scatter plot matrix is a grid (or matrix) of scatter plots used to visualize bivariate relationships between combinations of variables. Each scatter plot in the matrix visualizes the relationship between a pair of variables, allowing many relationships to be explored in one chart. In the upper diagonal, the distribution (histogram) of each variable difference is represented.

Figure 5

Scatter plot matrix of the VBD differences obtained from CEM and DM/DBT images and their relationship with all the other variable differences considered as independent in the multiple regression model: breast volume, volume of glandular tissue, breast thickness, compression force and pressure, contact area, nipple-to-posterior-edge distance, and mean glandular dose.

The only parameter the VBD difference can be considered more than very weakly correlated to is the difference in volume of glandular tissue ($r = 0.545$). Other correlations with moderate-to-strong relationships are recognizable between differences in breast volume and compressed breast thickness ($r = 0.708$), between breast volume differences and nipple-to-posterior-edge distance ($r = 0.667$), and finally between compression pressure differences and compression force differences ($r = 0.880$).

The Mann-Whitney test for independent samples applied to the subgroup of minimal or mild BPE compared with the subgroup of moderate or marked BPE did not show any statistically significant difference ($P = 0.1197$).

Discussion

The comparison between volumetric breast density measured in LE-CEM and in previous/subsequent DM or DBT images for the same patients did not find any statistically significant difference. This results was confirmed by the high correlation between the two VBD pairs for both per-view and per-case datasets, and with the Bland-Altman plots showing that the absolute difference between VBDs measured respectively in LE-CEM and in DM/DBT was very close to zero, with limits of agreement moving from ±8% in per-view analysis to ±6% in per-case analysis. This result suggests that VBD measured from LE-CEM images is comparable with VBD obtained from standard mammography or tomosynthesis images. Thereby, if CEM is used as detection tool, VBD measured using CEM can be used for risk evaluation as if it would be

obtained from mammography. This reinforces the substantial clinical equivalence between LE-CEM and mammography images, as published by Lalji and colleagues, who compared LE-CEM and DM image quality by applying EUREF clinical criteria [49].

Considering the VBD differences, the multiregression model showed that they are associated with variables related to breast compression (compression force and pressure, compressed breast thickness, and contact area) and with variables related to breast positioning (volume of glandular tissue and nipple-to-posterior-edge distance). As x-ray breast imaging, including mammography, tomosynthesis, and CEM requires manual breast compression and positioning by a breast radiographer, it is very hard, despite the application of criteria of “correct positioning”, to ensure that breast compression and positioning is the same for the same laterality and view for consecutive exams. In other words, despite the known advantages of using quantitative tools to evaluate breast density (compared to subjective categorization affected by intra- and inter-observer variability for the same exam), radiologists should be aware that reproducibility of breast density in two consecutive examinations can be subordinated to breast compression and positioning reproducibility. This topic has previously been explored by Alonzo-Proulx et al. in a small study of repositioning the left breast of 30 volunteers for a second CC view to evaluate the effect on measured density [50]. That study found a comparable VBD variability (between – 4.25% and 2.28%) as that observed here, even in the context of repositioning the breast on the same day and imaging on the same equipment. Such awareness of the potential sensitivity of density measurement to breast positioning is particularly important in case the quantitative breast density is used as decision making index to drive supplemental imaging or risk assessment in personalized screening programs. Breast density has shown to increase the accuracy of breast cancer risk models [9], but variability in breast density measures associated to changes in breast compression and positioning might have an impact in the predicted breast cancer risk. An investigation of breast positioning and compression quality is out of the scope of this work, but it is postulated that good breast positioning quality and consistent compression practices could mitigate the variability in automated density measurement, and subsequently the impact on breast cancer risk estimates.

Apart from breast positioning changes, the only other physical means by which the quantitative density on LE-CEM could be different than DM/DBT should be related to the potential presence of contrast agent in the breast tissue, and its influence on the image pixel magnitudes. BPE assessed on the subtracted image was used here as a surrogate estimate for the amount of normal tissue contrast agent uptake. The findings demonstrate no association between BPE and VBD difference, so it is estimated that the amount of iodine uptake in typical CEM produces signal intensity changes that are small enough as to not influence the density measurement method applied in this work.

This study has limitations: sample size was relatively small; all LE-CEM images were produced by the one type of equipment; DM images were not obtained at the same time as the CEM images. Nevertheless, the time interval between DM and CEM examinations (mean: 11 months; median: 12 months) was short enough to assume substantial temporal stability of breast density [51].

Conclusions

In conclusion, volumetric breast density can be obtained from contrast-enhanced spectral mammography (low-energy images), and is not significantly different from volumetric breast density values measured from standard mammograms, outside the inherent uncertainty associated with breast compression and positioning. This might become helpful if contrast-enhanced mammography will gain a role in personalization of screening programs.

Declarations

Ethics approval and consent to participate

Institutional Review Board approval was obtained for the study and informed consent was signed by all enrolled women (CE IOV #2017/92).

Consent for publication

Consent for publication was obtained from all the co-authors.

Availability of data and material

The dataset analysed during the current study is available from the corresponding author on reasonable request.

Competing interests

M.H. is a consultant of Volpara Health Technologies. The other authors of this manuscript declare no relationships with any companies whose products or services may be related to the subject matter of the article.

Funding

The clinical study from which the dataset used in this study was extracted received financial support by the Veneto Region (Grant Number: RSF-2017-00000562). There was not a specific grant for this study.

Authors' contributions

G.G. participated in work design, database management, data analysis, interpretation of data, manuscript draft. G.G. is the corresponding author.

M. H. participated in work design, interpretation of data, manuscript draft.

E.B. participated in database management and manuscript revision.

F.C. participated in work design, interpretation of data, manuscript draft and revision.

Acknowledgments

The authors thank Enrica Baldan for her contribution in women accrual, and Maria Petrioli and Tiziana Masiero for their effort in optimization of CEM exam acquisitions.

Abbreviations

CEM	contrast-enhanced mammography
LE	low-energy
HE	high-energy
DM	digital mammography
DBT	digital breast tomosynthesis
VBD	volumetric breast density

References

1. Day N, Warren R. Mammographic screening and mammographic patterns. Breast Cancer Res. 2000;2:4:247–51.
2. Mandelson MT, Oestreicher N, Porter PL, White D, Finder CA, Taplin SH, et al. Breast density as a predictor of mammographic detection: comparison of interval- and screen-detected cancers. J Natl Cancer Inst. 2000;92:13:1081–7.
3. Boyd NF, Martin LJ, Yaffe MJ, Minkin S. Mammographic density and breast cancer risk: current understanding and future prospects. Breast Cancer Res. 2011;13:6:223.
4. Soguel L, Durocher F, Tchernof A, Diorio C. Adiposity, breast density, and breast cancer risk: epidemiological and biological considerations. Eur J Cancer Prev. 2017;26:6:511–20.
5. Posso M, Louro J, Sanchez M, Roman M, Vidal C, Sala M, et al. Mammographic breast density: How it affects performance indicators in screening programmes? Eur J Radiol. 2019;110:81–7.
6. Gail MH, Pfeiffer RM. Breast Cancer Risk Model Requirements for Counseling, Prevention, and Screening. J Natl Cancer Inst. 2018;110:9:994–1002.
7. Lee A, Mavaddat N, Wilcox AN, Cunningham AP, Carver T, Hartley S, et al. BOADICEA: a comprehensive breast cancer risk prediction model incorporating genetic and nongenetic risk factors. Genet Med. 2019;21:8:1708–18.
8. Tyrer J, Duffy SW, Cuzick J. A breast cancer prediction model incorporating familial and personal risk factors. Stat Med. 2004;23:7:1111–30.
9. Brentnall AR, Harkness EF, Astley SM, Donnelly LS, Stavrinos P, Sampson S, et al. Mammographic density adds accuracy to both the Tyrer-Cuzick and Gail breast cancer risk models in a prospective UK screening cohort. Breast Cancer Res. 2015;17:1:147,015-0653-5.

10. Lee CI, Chen LE, Elmore JG. Risk-based Breast Cancer Screening: Implications of Breast Density. Med Clin North Am. 2017;101:4:725–41.
11. Destounis SV, Santacroce A, Arieno A. Update on Breast Density, Risk Estimation, and Supplemental Screening. AJR Am J Roentgenol. 2020;214:2:296–305.
12. Lian J, Li K. A Review of Breast Density Implications and Breast Cancer Screening. Clin Breast Cancer. 2020;20:4:283–90.
13. Spak DA, Plaxco JS, Santiago L, Dryden MJ, Dogan BE. BI-RADS((R)) fifth edition: A summary of changes. Diagn Interv Imaging. 2017;98:3:179–90.
14. Ciatto S, Houssami N, Apruzzese A, Bassetti E, Brancato B, Carozzi F, et al. Categorizing breast mammographic density: intra- and interobserver reproducibility of BI-RADS density categories. Breast. 2005;14:4:269–75.
15. Sacchetto D, Morra L, Agliozzo S, Bernardi D, Bjorklund T, Brancato B, et al. Mammographic density: Comparison of visual assessment with fully automatic calculation on a multivendor dataset. Eur Radiol. 2016;26:1:175–83.
16. Highnam R, Jeffreys M, McCormack V, Warren R, Davey Smith G, Brady M. Comparing measurements of breast density. Phys Med Biol. 2007;52:19:5881–95.
17. Yaffe MJ. Mammographic density. Measurement of mammographic density. Breast Cancer Res. 2008;10:3:209.
18. Keller BM, Chen J, Daye D, Conant EF, Kontos D. Preliminary evaluation of the publicly available Laboratory for Breast Radiodensity Assessment (LIBRA) software tool: comparison of fully automated area and volumetric density measures in a case-control study with digital mammography. Breast Cancer Res. 2015;17:117,015-0626-8..
19. Gastounioti A, Kasi CD, Scott CG, Brandt KR, Jensen MR, Hruska CB, et al. Evaluation of LIBRA Software for Fully Automated Mammographic Density Assessment in Breast Cancer Risk Prediction. Radiology. 2020;296:1:24–31.
20. Ekpo EU, McEntee MF. Measurement of breast density with digital breast tomosynthesis–a systematic review. Br J Radiol. 2014;87:1043:20140460.
21. Blake GM, Fogelman I. Technical principles of dual energy x-ray absorptiometry. Semin Nucl Med. 1997;27:3:210–28.
22. Manji F, Wang J, Norman G, Wang Z, Koff D. Comparison of dual energy subtraction chest radiography and traditional chest X-rays in the detection of pulmonary nodules. Quant Imaging Med Surg. 2016;6(1):1–5.
23. McCollough CH, Leng S, Yu L, Fletcher JG. Dual- and Multi-Energy CT: Principles, Technical Approaches, and Clinical Applications. Radiology. 2015;276:3:637–53.
24. Patel BK, Lobbes MBI, Lewin J. Contrast Enhanced Spectral Mammography: A Review. Semin Ultrasound CT MR. 2018;39:1:70–9.

25. Lalji U, Lobbes M. Contrast-enhanced dual-energy mammography: a promising new imaging tool in breast cancer detection. Womens Health (Lond). 2014;10:3:289–98.
26. Gilbert FJ, Pinker-Domenig K. Diagnosis and Staging of Breast Cancer: When and How to Use Mammography, Tomosynthesis, Ultrasound, Contrast-Enhanced Mammography, and Magnetic Resonance Imaging. In: Hodler J, Kubik-Huch RA, von Schulthess GK, editors. Diseases of the Chest, Breast, Heart and Vessels 2019–2022: Diagnostic and Interventional Imaging. Cham (CH): The Author(s); 2019. pp. 155–66.
27. Skarpathiotakis M, Yaffe MJ, Bloomquist AK, Rico D, Muller S, Rick A, et al. Development of contrast digital mammography. Med Phys. 2002;29:10:2419–26.
28. Lobbes MB, Smidt ML, Houwers J, Tjan-Heijnen VC, Wildberger JE. Contrast enhanced mammography: techniques, current results, and potential indications. Clin Radiol. 2013;68:9:935–44.
29. Fallenberg EM, Dromain C, Diekmann F, Engelken F, Krohn M, Singh JM, et al. Contrast-enhanced spectral mammography versus MRI: Initial results in the detection of breast cancer and assessment of tumour size. Eur Radiol. 2014;24:1:256–64.
30. Dromain C, Balleyguier C, Adler G, Garbay JR, Delaloge S. Contrast-enhanced digital mammography. Eur J Radiol. 2009;69:1:34–42.
31. Dromain C, Thibault F, Diekmann F, Fallenberg EM, Jong RA, Koomen M, et al. Dual-energy contrast-enhanced digital mammography: initial clinical results of a multireader, multicase study. Breast Cancer Res. 2012;14:3:R94.
32. Fallenberg EM, Schmitzberger FF, Amer H, Ingold-Heppner B, Balleyguier C, Diekmann F, et al. Contrast-enhanced spectral mammography vs. mammography and MRI - clinical performance in a multi-reader evaluation. Eur Radiol. 2017;27:7:2752–64.
33. Blum KS, Rubbert C, Mathys B, Antoch G, Mohrmann S, Obenauer S. Use of contrast-enhanced spectral mammography for intramammary cancer staging: preliminary results. Acad Radiol. 2014;21:11:1363–9.
34. Iotti V, Ravaioli S, Vacondio R, Coriani C, Caffarri S, Sghedoni R, et al. Contrast-enhanced spectral mammography in neoadjuvant chemotherapy monitoring: a comparison with breast magnetic resonance imaging. Breast Cancer Res. 2017;19:1:106,017-0899-1.
35. Tennant SL, James JJ, Cornford EJ, Chen Y, Burrell HC, Hamilton LJ, et al. Contrast-enhanced spectral mammography improves diagnostic accuracy in the symptomatic setting. Clin Radiol. 2016;71:11:1148–55.
36. Lobbes MB, Lalji U, Houwers J, Nijssen EC, Nelemans PJ, van Roozendaal L, et al. Contrast-enhanced spectral mammography in patients referred from the breast cancer screening programme. Eur Radiol. 2014;24:7:1668–76.
37. Houben IPL, Van de Voorde P, Jeukens CRLPN, Wildberger JE, Kooreman LF, Smidt ML, et al. Contrast-enhanced spectral mammography as work-up tool in patients recalled from breast cancer screening has low risks and might hold clinical benefits. Eur J Radiol. 2017;94:31–7.

38. Mori M, Akashi-Tanaka S, Suzuki S, Daniels MI, Watanabe C, Hirose M, et al. Diagnostic accuracy of contrast-enhanced spectral mammography in comparison to conventional full-field digital mammography in a population of women with dense breasts. Breast Cancer. 2017;24:1:104–10.
39. Sorin V, Yagil Y, Yosepovich A, Shalmon A, Gotlieb M, Neiman OH, et al. Contrast-Enhanced Spectral Mammography in Women With Intermediate Breast Cancer Risk and Dense Breasts. AJR Am J Roentgenol. 2018;211(5):W267-74.
40. Sung JS, Lebron L, Keating D, D'Alessio D, Comstock CE, Lee CH, et al. Performance of Dual-Energy Contrast-enhanced Digital Mammography for Screening Women at Increased Risk of Breast Cancer. Radiology. 2019;293:1:81–8.
41. Cuzick J. IBIS Breast Cancer Risk Evaluation Tool [Internet]. 2017.
42. Clinical Guidelines NICE, No. 164. **Familial breast cancer**: **classification**, **care and managing breast cancer and related risks in people with a family history of breast cancer**: National Institute for Health and Care Excellence (UK); 2019.
43. Branderhorst W, de Groot JE, van Lier MGJTB, Highnam RP, den Heeten GJ, Grimbergen CA. Technical Note: Validation of two methods to determine contact area between breast and compression paddle in mammography. Med Phys. 2017;44:8:4040–4.
44. Waade GG, Danielsen AS, Holen AS, Larsen M, Hanestad B, Hopland NM, et al. Assessment of breast positioning criteria in mammographic screening: Agreement between artificial intelligence software and radiographers. J Med Screen. 2021:969141321998718.
45. Dance DR, Skinner CL, Young KC, Beckett JR, Kotre CJ. Additional factors for the estimation of mean glandular breast dose using the UK mammography dosimetry protocol. Phys Med Biol. 2000;45:11:3225–40.
46. Dance DR, Young KC, van Engen RE. Further factors for the estimation of mean glandular dose using the United Kingdom, European and IAEA breast dosimetry protocols. Phys Med Biol. 2009;54:14:4361–72.
47. Dance DR, Young KC. Estimation of mean glandular dose for contrast enhanced digital mammography: factors for use with the UK, European and IAEA breast dosimetry protocols. Phys Med Biol. 2014;59:9:2127–37.
48. Sogani J, Morris EA, Kaplan JB, D'Alessio D, Goldman D, Moskowitz CS, et al. Comparison of Background Parenchymal Enhancement at Contrast-enhanced Spectral Mammography and Breast MR Imaging. Radiology. 2017;282:1:63–73.
49. Lalji UC, Jeukens CR, Houben I, Nelemans PJ, van Engen RE, van Wylick E, et al. Evaluation of low-energy contrast-enhanced spectral mammography images by comparing them to full-field digital mammography using EUREF image quality criteria. Eur Radiol. 2015;25:10:2813–20.
50. Alonzo-Proulx O, Mawdsley GE, Patrie JT, Yaffe MJ, Harvey JA. Reliability of automated breast density measurements. Radiology. 2015;275:2:366–76.
51. Shia WC, Wu HK, Huang YL, Lin LS, Chen DR. Mammographic Density Distribution of Healthy Taiwanese Women and its Naturally Decreasing Trend with Age. Sci Rep. 2018;8(1):14937,018–

32923.

Figures

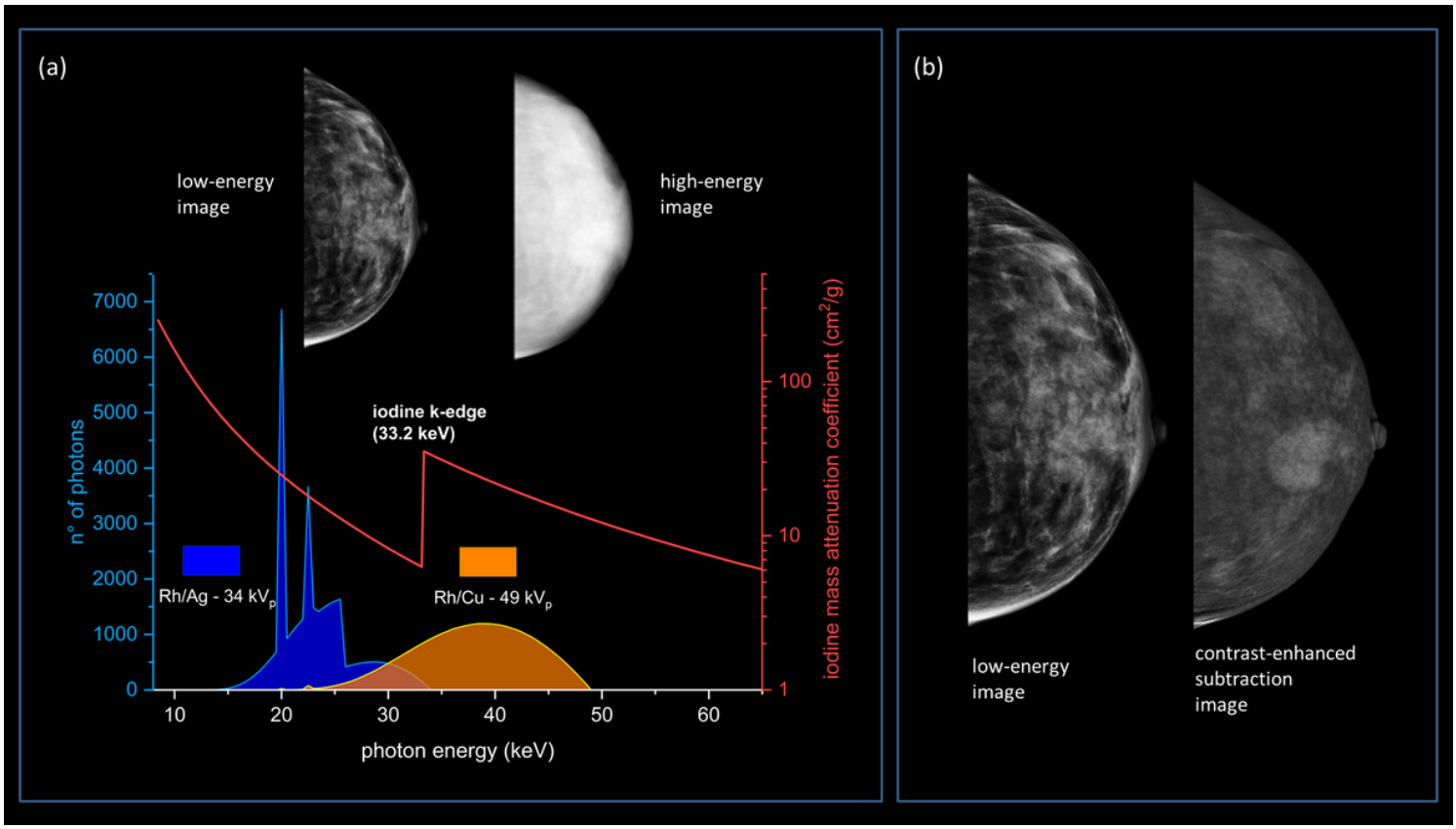

Figure 1

(a) CEM acquisition. Two minutes after the administration of iodinated contrast agent, for each mammography view an image pair is acquired: a low-energy image (LE-CEM) using an x-ray spectrum similar to that used to obtain a standard mammogram, and a high-energy image (HE-CEM) using a spectrum obtained with appropriate filtration and high tube voltage such as photon energies are mostly above the iodine k-edge (33.2 keV). (b) CEM interpretation. The LE-CEM is used for the morphological information and the contrast-enhanced subtraction image used as functional imaging; the HE-CEM image is not useful for diagnosis.

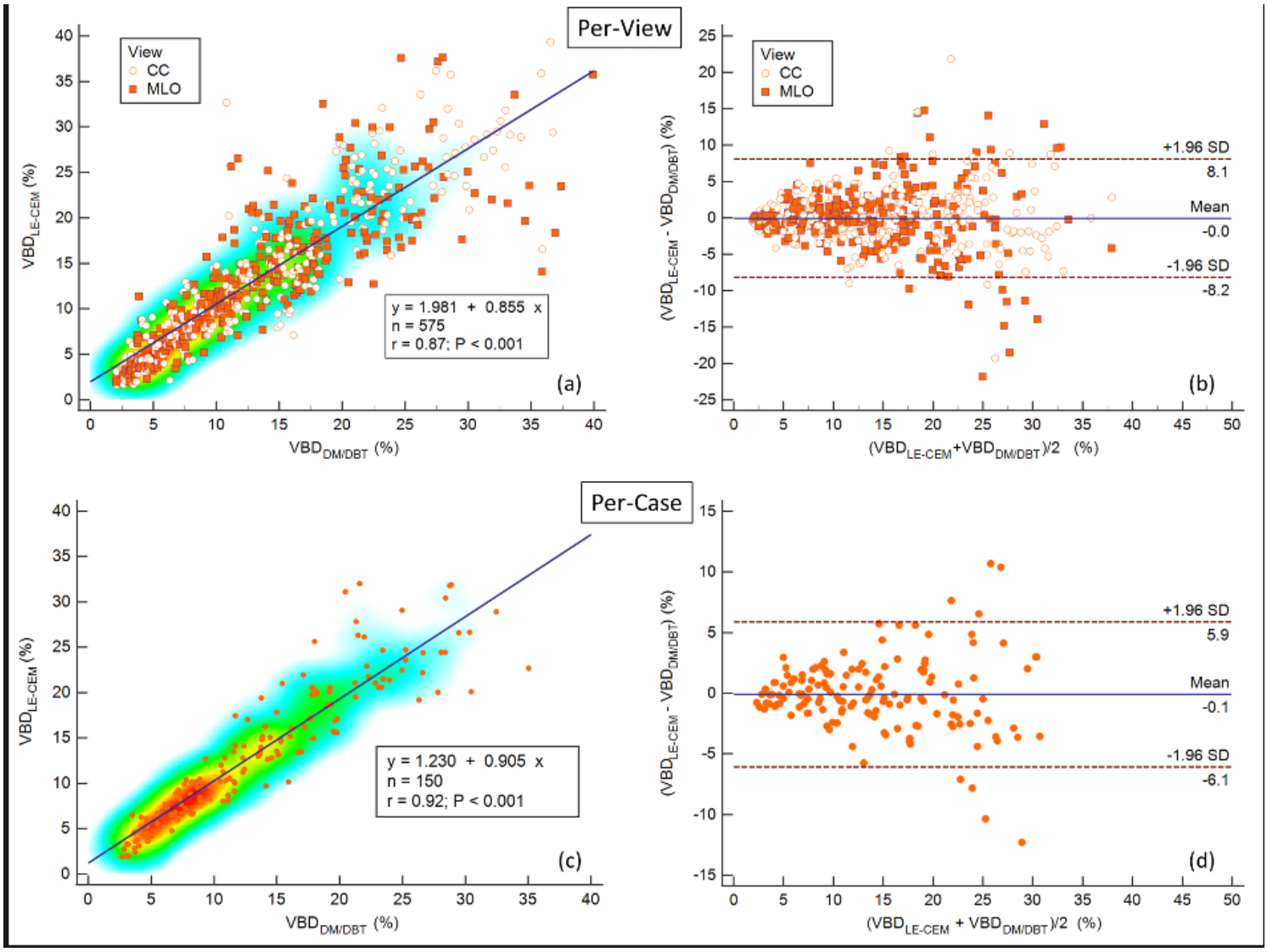

Figure 2

(a) Correlation plot of VBD measured in paired views obtained from LE-CESM and previous/subsequent DM/DBT exams; the Pearson's correlation coefficient was r=0.87, a reduction of correlation can be noticed as VBD increases, especially for MLO views. (b) Bland-Altman plot of VBD difference between LE-CESM and previous/subsequent DM/DBT for each paired view; the mean difference was zero, the limits of agreement ±,8%. (c) Correlation plot of mean VBD obtained by averaging single-view VBDs for each paired study obtained with LE-CESM and DM/DBT; the Pearson's correlation coefficient was r=0.92, the heat map shows that VBD values were mostly grouped below 15%. (d) Bland-Altman plot of VBD difference between LE-CESM and previous/subsequent DM/DBT for each paired study; the mean difference was confirmed to be very close to zero, the limits of agreement reduced to ±,5%.

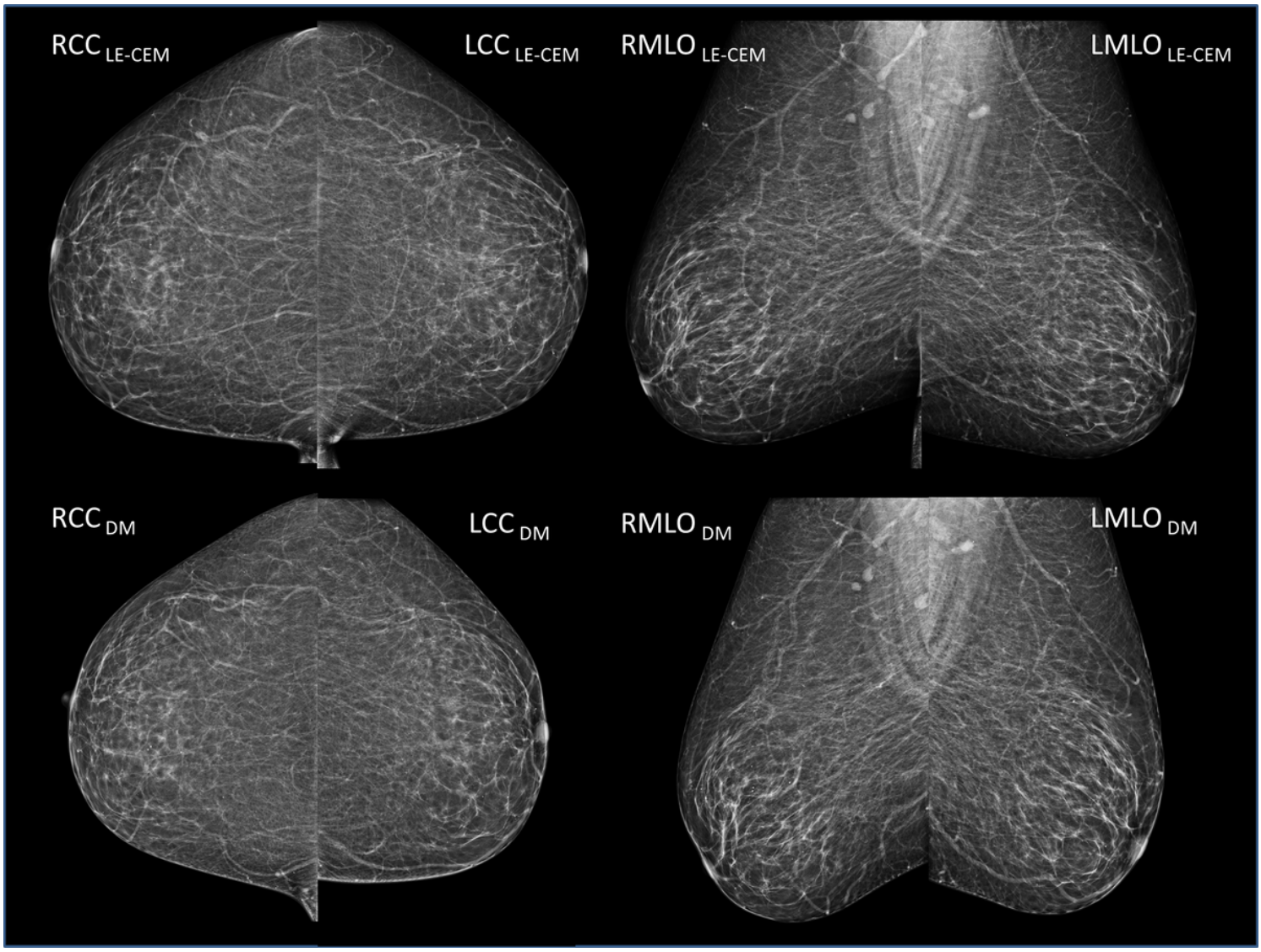

Figure 3

(Upper row) LE-CEM images of a woman with large fatty breasts. VBD: 1.9%; breast volume: 2634 cm3; volume of glandular tissue: 51 cm3; breast thickness: 85 mm; nipple-to-posterior-edge distance: 174 mm. (Lower row) DM images acquired 12 months before the CEM exam. VBD: 2.7%: breast volume: 2058 cm3; volume of glandular tissue: 54 cm3; breast thickness: 76 mm; nipple-to-posterior-edge distance: 155 mm. Despite the visible difference in breast positioning, the large reduction in breast volume due to worse positioning in the DM exam did not produce a significant variation of breast density, being the breasts predominantly fatty.

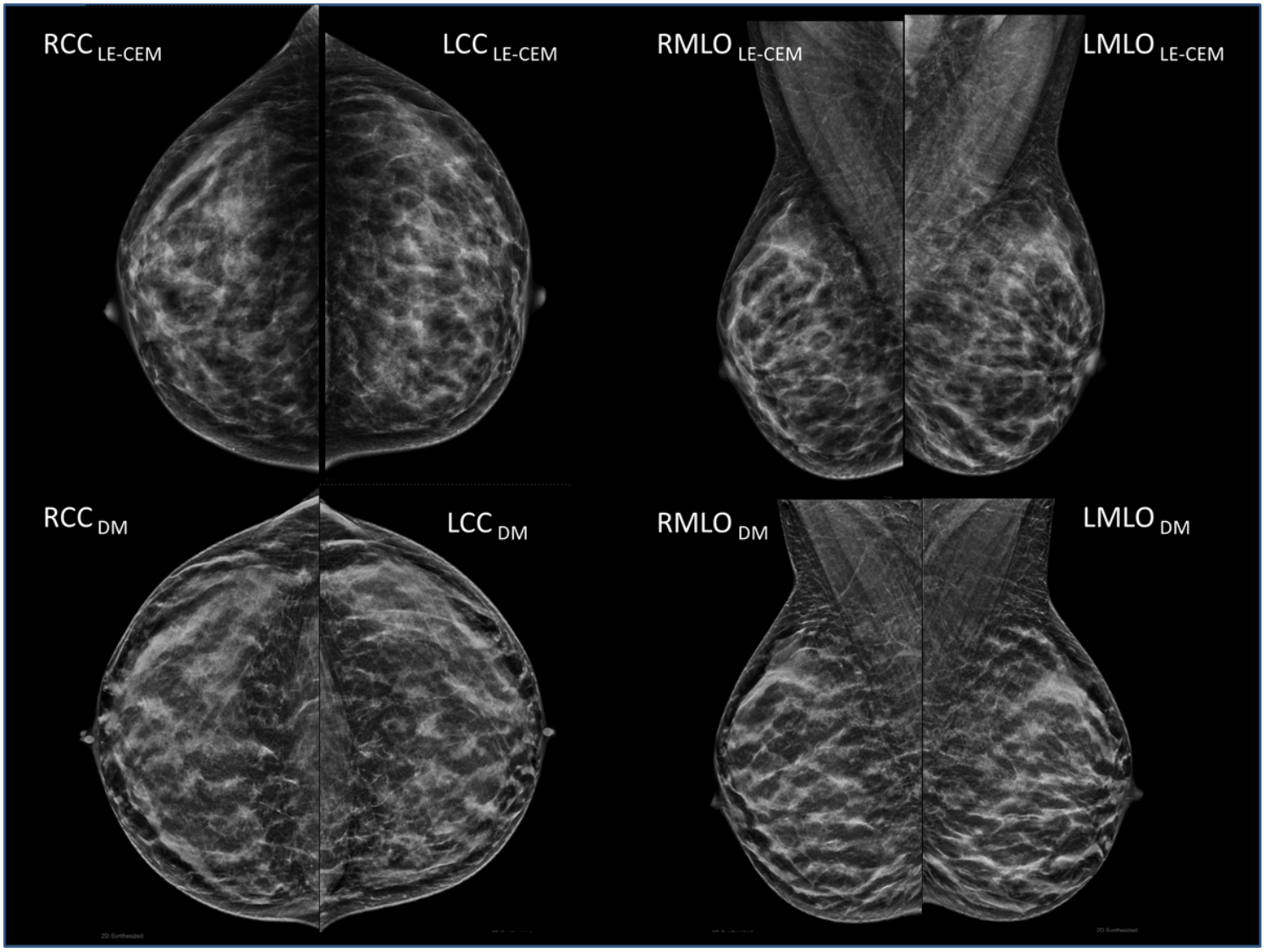

Figure 4

(Upper row) LE-CEM images of a woman with dense breasts. VBD: 20.1%; breast volume: 319 cm3; volume of glandular tissue: 64 cm3; breast thickness: 32 mm; nipple-to-posterior-edge distance: 86 mm. (Lower row) DM images acquired 11.5 months after the CEM exam. VBD: 30.5%; breast volume: 450 cm3; volume of glandular tissue: 136 cm3; breast thickness: 41 mm; nipple-to-posterior-edge distance: 98 mm. Breast positioning is better in DM exam, including an additional volume of glandular tissue leading to a significant increment in VBD.

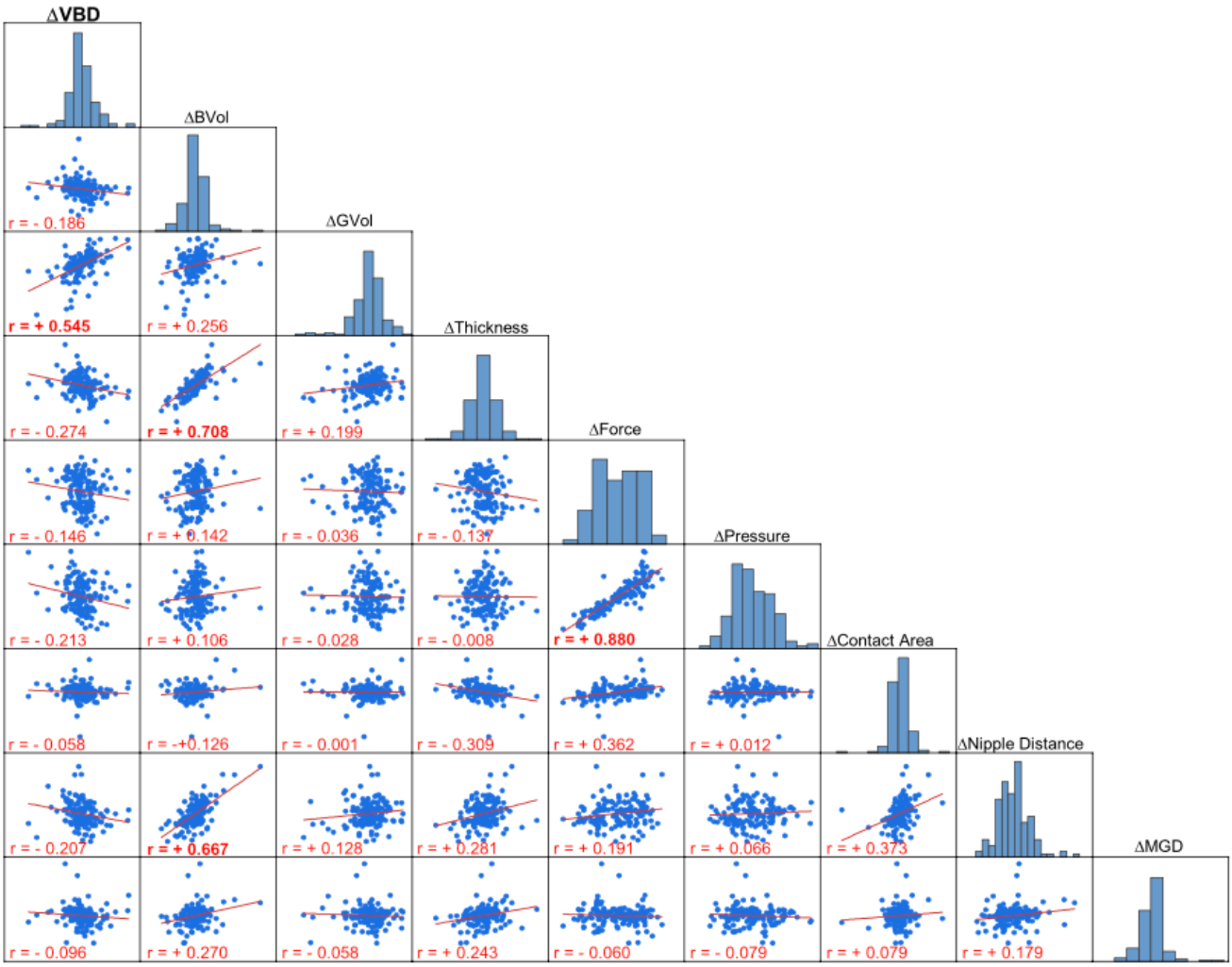

Figure 5

Scatter plot matrix of the VBD differences obtained from CEM and DM/DBT images and their relationship with all the other variable differences considered as independent in the multiple regression model: breast volume, volume of glandular tissue, breast thickness, compression force and pressure, contact area, nipple-to-posterior-edge distance, and mean glandular dose.